Supplemental Data

Figure S1

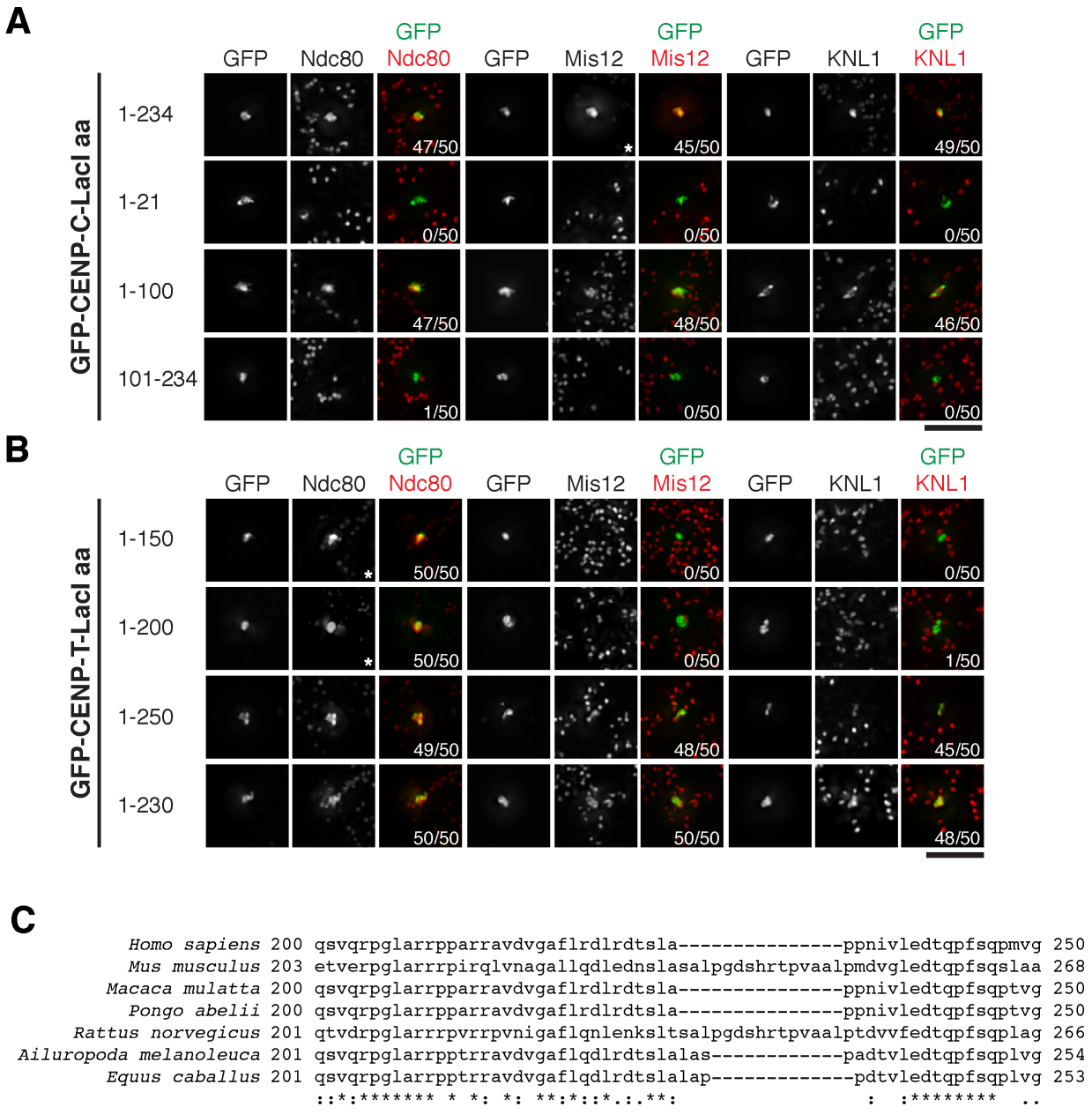

Figure S1: CENP-C recruitment of KMN network proteins occurs at the N-terminus and CENP-T recruits Ndc80 and KNL1/Mis12 via two separate domains. Related to Figure 1. A) Representative immunofluorescence images showing the GFP-CENP-C-LacI foci stained for each of the corresponding KMN network components in mitotic cells arrested using nocodazole. Images of Ndc80 localization for CENP-C aa 1-100 and 101-234 were replicated from Figure

1A. All images were scaled independently to show the full range of the data. Images marked with * were scaled in gamma. Numbers in lower right corner indicate number of mitotic cells out of 50 that showed co-localization between the GFP focus and the indicated test protein. B) Representative immunofluorescence images showing localization of the GFP-CENP-T-LacI foci as well each of the corresponding KMN network components in mitotic cells arrested using nocodazole. All images were scaled independently to show the full range of the data. Images marked with * were scaled in gamma. Numbers in lower right corner indicate number of mitotic cells out of 50 that showed co-localization between the GFP focus and indicated test protein. C) Alignment of CENP-T from the indicated species was performed using Clustal Omega [S1]. Scale bars, 5 μm.

Figure S2

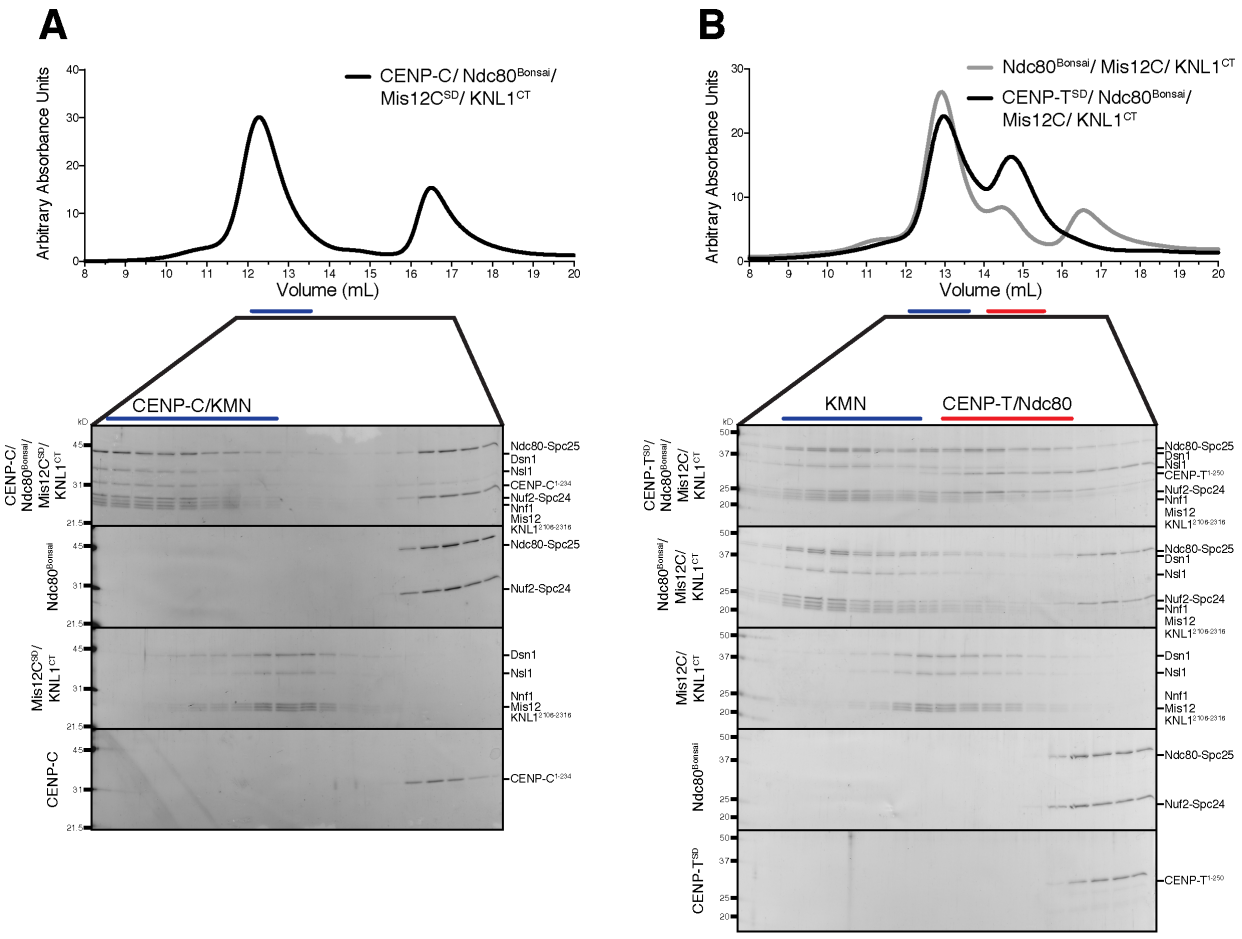

Figure S2: Binding of KMN network components to CENP-C and CENP-T in vitro. Related to Figure 1. A) Top: Size exclusion chromatography elution profile of CENP-C^{1-234}, $Ndc80^{Bonsai}$, $Mis12C^{SD}$, $KNL1^{2106-2316}$ purified from bacteria. Bottom: SDS-PAGE of equivalent fractions for the indicated proteins, in combination and separately. B) Top: Size exclusion chromatography elution profile of recombinant purified CENP-T^{SD}(1-250), $Ndc80^{Bonsai}$, Mis12C, $KNL1^{2106-2316}$ (black) and $Ndc80^{Bonsai}$, Mis12C, $KNL1^{2106-2316}$ (gray) purified from bacteria. Bottom: SDS-PAGE of equivalent fractions for the indicated proteins, in combination and separately.

Figure S3

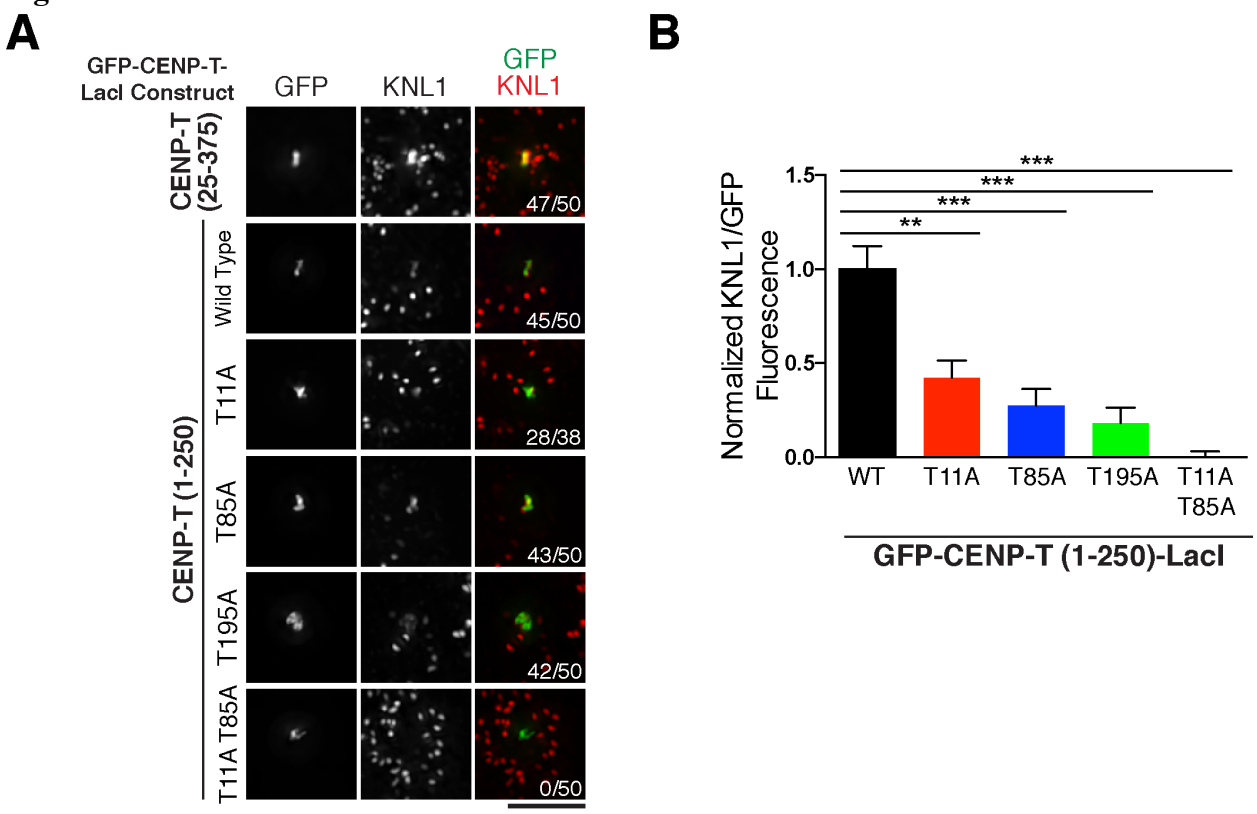

Figure S3: Analysis of KNL1 localization to CENP-T phospho-mutant foci. Related to Figure 3. A) Representative immunofluorescence images showing GFP-CENP-T-LacI foci co-stained for KNL1 in nocodazole-treated cells. All images were scaled independently to show the full range of the data. Numbers in lower right corner indicate the number of mitotic cells that showed co-localization between the GFP focus and KNL1. The images for the wild type CENP-T 1-250 construct are duplicated from Figure S1. Scale bar, 5 μm. B) Graph showing the average ratio KNL1/GFP fluorescence (+/- SEM) for the indicated GFP-CENP-T-LacI foci (N = 10 cells/condition). Student's t-test - **: $p<0.01$; ***: $p<0.001$.

Figure S4

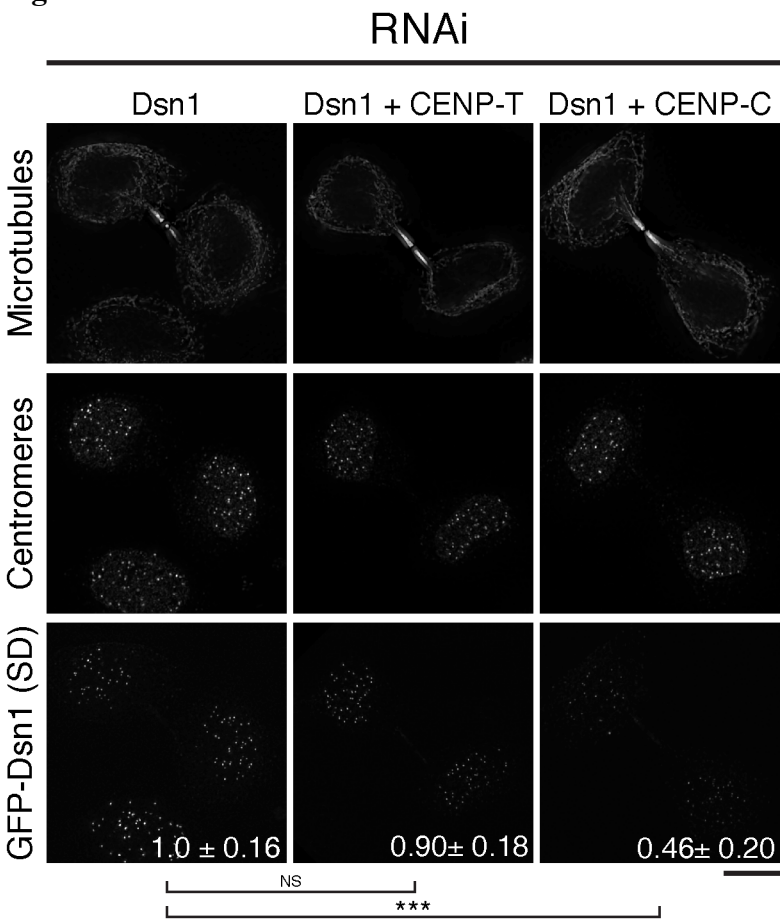

Figure S4: Dsn1 Aurora B mutants require CENP-C for their interphase localization. Related to Figure 4. Representative immunofluorescence images showing the localization of the GFP-Dsn1 Aurora B phosphomimetic (SD; S28D, S78D, S100D, S109D) mutant in G1 cells. Cells were depleted of endogenous Dsn1, and were additionally co-depleted for CENP-C or CENP-T as indicated. Cells were probed with antibodies against centromeres (ACA) and microtubules (DM1alpha). Microtubule staining is scaled in gamma to visualize the range of data. Numbers indicate the fluorescence intensity of the GFP-Dsn1 mutant relative to cells depleted for endogenous Dsn1 alone. 20 G1 cells pairs were quantified for each condition. Student's t-test - NS: not significant, ***: $p<0.001$. Scale bar, 10 μM.

Supplemental Experimental Procedures

Cell Culture

U2OS *lacO* [S2] and HeLa cell lines were cultured in DMEM supplemented with 10% FBS, penicillin/streptomycin, and 2 mM L-glutamine. U2OS cells were maintained in 10 mM IPTG and 0.25 mg/mL Hygromycin B (Invitrogen). IPTG was washed out 24 (Fig. 1, 3B, 3C, 4A, 4B, S1A, S1B, S3), 48 (2A, 2B), or 72 (3D, 3E) hr prior to fixation to allow recruitment of the LacI fusions to the *lacO* array. Where indicated, U2OS cells were incubated in 330 nM nocodazole for 14 hr to enrich for mitotic cells. For Aurora B kinase inhibition assays, cells were incubated in 2 μM ZM447439 (Tocris Bioscience) for 2 – 2.5 hr prior to fixation.

Cell Line Generation and Transfection

Clonal cell lines stably expressing GFP^{LAP} fusions were generated in U2OS *lacO* and HeLa cells as previously described [S3]. RNAi resistant CENP-T and CENP-C used for fusion cloning were described previously [S4]. Phosphomutants were generated using site-directed mutagenesis. All indicated truncations were generated by cloning into a GFP^{LAP}-X-LacI backbone [S4]. Small interfering RNAs (siRNAs) against Nuf2 (5'-AAGCAUGCCGUGAAACGUAUAUU-3') [S5], Dsn1 (5'-GGAAACUGAUGGAACUCUA-3', 5'-GGAGAUGAAUCAAGGCGUU, GAUCAUCAAUUGGAAUCAA-3', 5'-GCGGCGAGCAAGUAUGAAA-3') [S6], KNL1 (5'-GGAAUCCAAUGCUUUGAGA-3') [S7], CENP-T (5'-CGGAGAGCCCUGCUUGAAA-3') [S4], CENP-C (5'- GAACAGAAUCCAUCACAAA-3') [S4], and a nontargeting control were obtained from Dharmacon. siRNAs were transfected using Lipofectamine RNAi MAX and

serum-free OptiMEM (Invitrogen). DMEM plus 10% FBS was added after 6 hr and cells were fixed 48 hr after transfection.

Immunofluorescence and Microscopy

U2OS cells were pre-extracted for 3 minutes in PBS plus 0.1% Triton X-100 before fixation in 4% formaldehyde in PBS. HeLa cell lines in which mitotic populations were analyzed were pre-extracted for 5 minutes in PBS plus 0.5% Triton X-100 before fixation in 4% formaldehyde in PBS. In cases where G1 populations were being observed, pre-extraction was performed in PHEM (60 mM PIPES, 25 mM HEPES, 10 mM EGTA, 2 mM $MgCl_2$, pH 6.9) plus 0.5% Triton X-100, and subsequently fixed in 4% formaldehyde in PHEM. Ndc80 was detected using either mouse anti-Hec1 (9G3, Abcam; for Fig. 2A, 2B) or a polyclonal rabbit anti-$Ndc80^{Bonsai}$ against the entire Ndc80 complex ([S8]; for Fig. 1A, 1C, 3B, 3C, 4A, 4B, S1A, S1B). KNL1 was detected using polyclonal rabbit anti-$KNL1^{1413\text{-}1624}$ ([S7]; for Fig. 1C, 2A, 2B, 4A, 4B, S1A, S1B, S3) or a mouse anti-Blinkin ([S9]; for Fig. 2A and 2B). Affinity-purified rabbit polyclonal antibodies were generated against the complete Mis12 complex as described previously [S10]. CENP-A was detected using mouse anti-CENP-A (3-19) (Abcam). Human centromeres were detected using anti-centromere antibodies (ACA) (Antibodies, Inc.). Microtubules were detected with mouse DM1alpha (Sigma). Cy2-, Cy3- and Cy5-conjugated secondary antibodies were obtained from Jackson Laboratories. DNA was visualized using 10 μg/mL Hoechst.

Immunofluorescence images were acquired on a Nikon Eclipse Ti-E microscope equipped with an Andor Clara charge-coupled device (CCD) camera using the NIS-Elements AR software (v4.2). Z sections were acquired at 0.2 μm steps over 4 μm (U2OS cell lines) or 2 μm (for HeLa cell lines and U2OS cell lines in Fig. 3C and S3B) using a 60x/ 1.4 numerical aperture

(NA) Nikon Plan Apochromat λ objective plus 1.5x optovar. Images were deconvolved using the 3D Landweber deconvolution package accompanying NIS Elements when appropriate. Fluorescent images of focus segregation were acquired on a DeltaVision Core deconvolution microscope (Applied Precision) equipped with a CoolSnap HQ2 CCD camera with approximately 10 Z-sections acquired at 0.2 μm steps using a 60×/ 1.42 NA Olympus U-PlanApo objective and deconvolved using DeltaVision software. Images are scaled equivalently when shown for comparison, unless otherwise stated. Quantification of fluorescence intensity was conducted on unprocessed images using Metamorph (Molecular Devices). Due to the irregularity in GFP focus size and brightness, normalization was performed by measuring the intensity of the entire focus area for each channel over background. A ratio of test protein/GFP intensity was then calculated and averaged.

Protein Expression and Purification

Proteins were purified using the previously described bacterial expression constructs for GST-Ndc80^{Bonsai} [S11], His-tagged full-length Mis12 complex [S6], which was co-expressed with KNL1$^{2106-2316}$ cloned as described previously [S12] and GST-CENP-C$^{1-234}$ [S4]. CENP-T$^{1-250}$ was His-tagged by PCR and then cloned into pET3aTr. Phospho-mimetic mutations were introduced into the appropriate expression constructs (CENP-T T11, T27, S47, T85, T195 [Fig. S2B] ; Dsn1 [Fig. S2A] S28, S30, S58, S76, S80, S100, S109, S330) using site-directed mutagenesis. To purify GST-tagged proteins, bacteria were lysed in PBS, 250 mM NaCl, 0.1% Tween-20 and the lysate was bound to glutathione agarose (Sigma) for 1 hr at 4 °C. The resin was washed three times with PBS, 250 mM NaCl, 0.1% Tween-20, and 1 mM DTT. The proteins were then cleaved off the beads by overnight cleavage with PreScission protease at 4 °C. All His-tagged

proteins were purified by Ni-NTA affinity purification. Bacteria were lysed in 50 mM sodium phosphate buffer (NaPi), pH 8.0, 300 mM NaCl, 10 mM imidazole, 5 mM beta-mercaptoethanol (βME) and then incubated with Ni-NTA agarose (Qiagen) for 1 hr at 4 °C. The resin was washed three times with 50 mM NaPi, pH 8.0, 500 mM NaCl, 40 mM imidazole, 5 mM βME, followed by elution with 50 mM NaPi, 500 mM NaCl, 250 mM imidazole, 5 mM βME. All proteins were further purified by gel filtration on a Superdex 200 column into 50 mM Tris, pH 7.6, 150 mM NaCl, 1 mM DTT. Peak fractions were pooled and concentrated using Vivaspin 20 concentrators and snap frozen in liquid nitrogen.

Protein Binding Assays

Protein binding was assessed by mixing the appropriate proteins at final concentrations of 3 μM each in a final volume of 250 μl and incubating for 15 min on ice, followed by a 15 min spin at 4 °C at > 20,000 x g to remove any aggregates. The cleared supernatant was applied to a Superose 6 10/300 column in 50 mM Tris, pH 7.6, 150 mM NaCl, 1 mM DTT, and the peak fractions were analyzed on acrylamide gels and visualized using Coomassie R-250.

Supplemental References

S1. McWilliam, H., Li, W., Uludag, M., Squizzato, S., Park, Y. M., Buso, N., Cowley, A. P., and Lopez, R. (2013). Analysis Tool Web Services from the EMBL-EBI. Nucleic Acids Res *41*, W597–600.

S2. Janicki, S. M., Tsukamoto, T., Salghetti, S. E., Tansey, W. P., Sachidanandam, R., Prasanth, K. V., Ried, T., Shav-Tal, Y., Bertrand, E., Singer, R. H., et al. (2004). From Silencing to Gene Expression. Cell *116*, 683–698.

S3. Cheeseman, I. M., Niessen, S., Anderson, S., Hyndman, F., Yates, J. R., Oegema, K., and Desai, A. (2004). A conserved protein network controls assembly of the outer kinetochore and its ability to sustain tension. Genes Dev *18*, 2255–2268.

S4. Gascoigne, K. E., Takeuchi, K., Suzuki, A., Hori, T., Fukagawa, T., and Cheeseman, I. M. (2011). Induced Ectopic Kinetochore Assembly Bypasses the Requirement for CENP-A Nucleosomes. Cell *145*, 410–422.

S5. DeLuca, J. G., Moree, B., Hickey, J. M., Kilmartin, J. V., and Salmon, E. D. (2002). hNuf2 inhibition blocks stable kinetochore-microtubule attachment and induces mitotic cell death in HeLa cells. J. Cell Biol. *159*, 549–555.

S6. Kline, S. L., Cheeseman, I. M., Hori, T., Fukagawa, T., and Desai, A. (2006). The human Mis12 complex is required for kinetochore assembly and proper chromosome segregation. J. Cell Biol. *173*, 9–17.

S7. Cheeseman, I. M., Hori, T., Fukagawa, T., and Desai, A. (2008). KNL1 and the CENP-H/I/K complex coordinately direct kinetochore assembly in vertebrates. Mol. Biol. Cell *19*, 587–594.

S8. Schmidt, J. C., Arthanari, H., Boeszoermenyi, A., Dashkevich, N. M., Wilson-Kubalek, E. M., Monnier, N., Markus, M., Oberer, M., Milligan, R. A., Bathe, M., et al. (2012). The kinetochore-bound Ska1 complex tracks depolymerizing microtubules and binds to curved protofilaments. Developmental Cell *23*, 968–980.

S9. Kiyomitsu, T., Obuse, C., and Yanagida, M. (2007). Human Blinkin/AF15q14 Is Required for Chromosome Alignment and the Mitotic Checkpoint through Direct Interaction with Bub1 and BubR1. Developmental Cell *13*, 663–676.

S10. Desai, A., Rybina, S., Müller-Reichert, T., Shevchenko, A., Shevchenko, A., Hyman, A., and Oegema, K. (2003). KNL-1 directs assembly of the microtubule-binding interface of the kinetochore in C. elegans. Genes Dev *17*, 2421–2435.

S11. Ciferri, C., Pasqualato, S., Screpanti, E., Varetti, G., Santaguida, S., Reis, Dos, G., Maiolica, A., Polka, J., De Luca, J. G., De Wulf, P., et al. (2008). Implications for kinetochore-microtubule attachment from the structure of an engineered Ndc80 complex. Cell *133*, 427–439.

S12. Petrovic, A., Pasqualato, S., Dube, P., Krenn, V., Santaguida, S., Cittaro, D., Monzani, S., Massimiliano, L., Keller, J., Tarricone, A., et al. (2010). The MIS12 complex is a protein interaction hub for outer kinetochore assembly. The Journal of Cell Biology *190*, 835–852.